AN In-SAS SYSTEM FOR SHALLOW WATER SURVEYING

Sergio Rui Silva, Sergio Reis Cunha, Anbal Matos, Nuno Cruz
Faculty of Engineering of Porto University, CIIMAR
srui@fe.up.pt

Keywords: In-SAS, sonar, autonomous boat.

Abstract

This paper describes a SAS (Synthetic Aperture Sonar) system that is being developed at the University of Porto. This system is operated from an autonomous small boat and enables mapping of submerged bottoms of rivers, deltas, estuaries, dams and lakes. The focus of this paper is on the design features, principles of operation, the hardware and the target applications and on the project status.

1 Introduction

Like in SAR (Synthetic Aperture Radar), a SAS system explores the combined processing of a set of sent/received signals by a probe that moves relatively to targets of static nature, to generate high resolution images. The target distinction capacity rests in the sophistication of the transmitted signal and in the processing of sequence of the received waveforms of the resulting target echoes. Comparatively to real narrow aperture systems, the required hardware is simpler, allowing for a low cost solution.

Once in production, this system will enable mapping and characterization of low depth stream beds, being able to be used in rivers, estuaries, lakes, etc. Its contribution to the study of these areas is of interest to science, economy and ecology related fields (infra-structure maintenance, sand extraction, river navigability, among others). The autonomous boat is described in another paper/presentation submitted to this conference. In short, it provides several hours of unmanned operation, fulfilling a pre-defined mission plan. Its size is suitable for, together with the navigation system, executing profiles and other maneuvers with sub-meter accuracy. This floating platform incorporates an acoustic transducer matrix, placed beneath the waterline, and a set of GPS receivers together with an inertial sensor to compute its position and attitude with high precision and time resolution. It also embodies an on-board computer for signal generation, as well as for acquisition and storage of data. The existing SAS systems are typically based on submersed platforms, hindering the use of satellite based navigation systems, which achieve today levels of accuracy unmatched in underwater environments. This reflects immediately on the quality of the results. The use of a floating platform brings satellite navigation possible. The described system relies on the precision obtained in the platform position and attitude through tight integration of GPS receivers (with carrier phase processing - CP-DGPS) with one inertial sensor to address the problems related to target discrimination and measurement errors. Knowing the position and attitude of the platform makes construction of three dimensional maps of the analyzed surfaces possible through interferometric processing of multiple images of the same scene (In-SAS, Interferometric SAS). The use of absolute coordinates also makes the task of data integration with other geographic information systems easier. The In-SAS system is based in a set of simple acoustic transducers operating around 200 KHz, corresponding to a wavelength of 0.75 cm. As appropriate for synthetic aperture operations, their real aperture is large (approximately 20 degrees). The effective transducer diameter is 2 cm, which allows for synthetic images with this order of magnitude of resolution in the along-track direction. In opposition to other systems, the usable bandwidth of the transducers (and of the signals employed) is greatly explored to obtain the highest possible resolution images obtainable from the system. The transducers are driven by a dedicated FPGA based system. This provides a low cost solution for generating the complex acoustic signals, for controlling the transmitting power amplifiers and the adaptive gain low noise receiving amplifiers, for demodulating and for match filtering the received signals. The results are then supplied to an embedded computer for storage and acoustic image computation. The whole system fits a small box, compatible with the autonomous boat both in size and low power consumption. The accuracy of the images depends heavily on the ability to correct sensor motion errors. The followed approach is to compensate for these with information from a high accuracy GPS+INS navigation system. The GPS system operates in carrier phase ambiguity resolution mode with a base station established in a nearby shore and provides also absolute heading estimates from

differential processing of two antennae on the boat. From integration with the inertial unit, a full high rate position, velocity and attitude navigation solution is obtained.

2 Hardware

The synthetic aperture sonar system presented in this document is constituted by an autonomous-boat and a broad beam, high frequency sonar system (Figures 1) . The autonomous boat serves as moving platform for the sonar, navigation system and on-board computer (Figure 2). The sonar is constituted by an array of broad beamwidth transducers, a power amplifier, a low noise gain controllable amplifier and a analogue-to-digital/digital-to-analogue conversion and processing subsystem integrated in a FPGA.

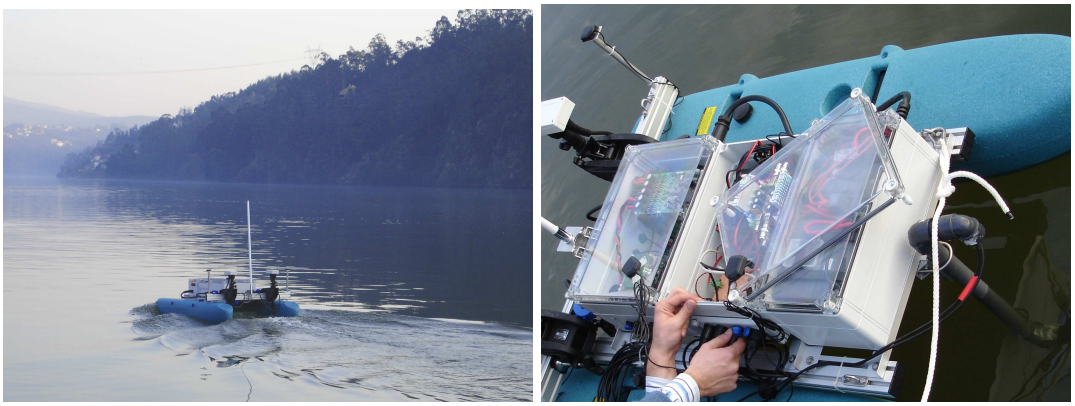

(a) Autonomous boat in operation. (b) Equipment present in the autonomous boat.

Figure 1: Autonomous boat.

The on-board PC collects the sonar and navigation data, relaying the obtained measurements to the mission control PC on in the shore or a nearby support boat for immediate supervision. The mission control PC has complete control of the several subsystems located in the autonomous boat. This is possible using a high speed digital wireless link that can be extended up to several kilometers and have a maximum throughput rate in the range of tens of Mbps. The collected data can also be stored in a hardisk onboard the boat. In addition, the mission control PC receives data from a GPS reference station, providing a refined navigation solution. Because the system is being designed for shallow water surveys, the short ranges enable the use of low power and high frequency transducers. These transducers have a broad conical 18 radiation beamwidth of about 18 degrees, a centre frequency of 200kHz, a usable bandwidth of 40kHz and allow 50W of peak power (about 222dB re 1Pa/V). After raw data processing with the image formation algorithm this system is capable of producing images with sub decimiter resoltution, both in along-track and cross-track directions.

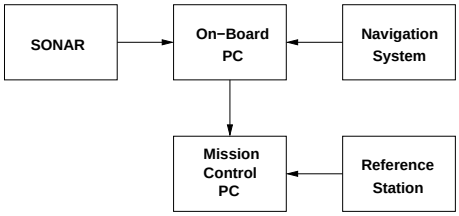

Figure 2: Sonar system overview.

The sonar system is based on direct-to-digital architecture (Figure 3), meaning that other than the transducers, only the power stage and pre-amplifier are implemented using analogue electronic components ([1], [2]). The system complexity stands, therefore, in the digital domain, enabling more flexible and higher quality signal acquisition and processing through a FPGA system. This system is being tailored for a high resolution interferometric synthetic aperture sonar. Special attention was paid to the different analogue components in terms of bandwidth, frequency amplitude response and phase linearity.

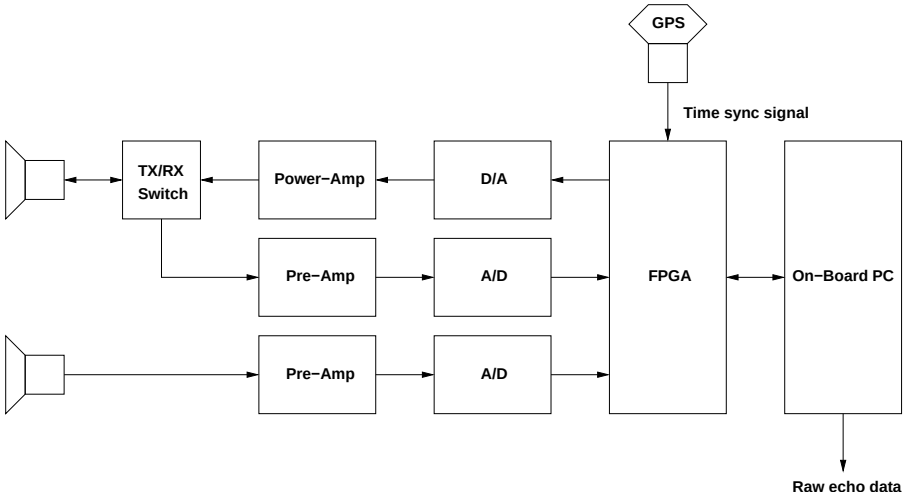

Figure 3: Sonar front-end.

The power-amplifier is a linear amplifier which can have a bandwidth of as high as 10MHz, and has a continuous output power rate of 25W (RMS). A trade-of was made between output power and bandwidth. Because we are interested in using our system in shallow waters, an output power of 25W was found to be adequate for this 200kHz sonar system. In exchange it was possible to build a power-amplifier with very flat amplitude and linear phase response in addition to low distortion (THD < -60dB) in the spectral band of interest. Each receiving channel has a low noise amplifier and a controllable gain amplifier to handle the high dynamic range of echo signals. The pre-amplifier system has a bandwidth of 10MHz, a noise figure of 2dB and a 50-115dB gain range. It can also recover rapidly from overdrive caused by the transmitting pulse. To reduced aliasing, a linear phase analogue filter is used in combination with a high sample rate A/D (up to 40MSamples/s). This anti-aliasing filter is interchangeable and can have a cut-off frequency of, for example, 650kHz or 2,3MHz. Both the D/A and A/D have 12 bit resolution and are capable of 200MSamples/s and 40MSamples/s respectively. The 12 bit resolution of the A/D (effective 72db SNR) was found to be high enough to cope with the front-end performance that is dominated by the transducers noise. The use of a FPGA system for signal acquisition enables a high control of the wave form that is being produced and the instant that it is being transmitted. It also makes the use of parallel processing (digital down-conversion, filtering, pulse-compression, etc) from several sources at high sample rates possible (Figure 4).

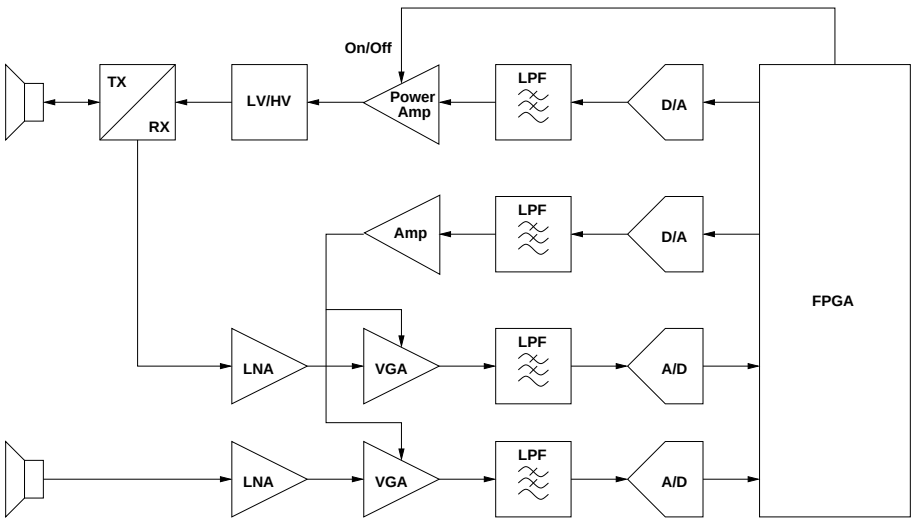

Figure 4: Sonar analogue front-end detail.

A dedicated GPS receiver serves as clock source for the real-time clock implemented in the FPGA, to control the pulse transmission and time-stamping of the received echoes. This clock uses a digital phase

lock loop that employs the GPS time data and the PPS signal to obtain a very stable and reliable clock source. This allows unambiguous correlation with the navigation data and thus, enhanced image quality through motion compensation algorithms. This system is hence adequate for use even with very high frequency transducers. The complete sonar system draws very small amout of power as necessary for its use in autonomous vehicles: 6W in standby mode versus 50W in transmit mode.

3 Raw data processing

To obtain a sonar image the system has to be able to generate, acquire and process raw signals and transform them into meaningful data. The generated output signal is recorded in a ROM table in the base-band domain and is digitally frequency up-converted in the FPGA using a controllable direct digital synthesizer (DDS). This signal has embedded the necessary system distortion and frequency response corrections. Although the digital-to-analogue converters and power amplifier have very good linear and frequency responses, the transducers do not; they have to be compensated in order to explore the largest possible bandwidth. The transmitted signal can be of any kind: linear chirp, logarithmic chirp or pseudo-random sequence. It can also have any suitable windowing function applied. Because of the efficient FPGA implementation, the system can also pair with large signal bandwidths ($>$ 100kHz) enabling high range resolution systems. At this moment, a linear chirp of 40 kHz bandwidth is being used for system tests. The system is prepared to output a pulse rate between 1 to 15Hz. Because we are interested in shallow water surveys, short ranges enable higher pulse rates. Nevertheless, because of the broad beamwidth of the transducer and its effective diameter, a pulse rate of 15Hz still imposes very low moving speeds to the autonomous boat (0,16m/s) that in turn has to couple with higher precision trajectory tracking constrains. This is of course a limitation that can be mitigated through various ways (higher number of array elements, use of orthogonal signals) and will be further studied ([4]), although preliminary simulations and tests show that a under-sampling factor as high as 20 can be perfectly amenabled (Figure 5) when using high bandwidth signals as in the case for the transmitting pulse employd ([3]). This is because when using high bandwidth signals the energy in the point target response side-bands is spread across the along track dimension instead of concentrating on specific points.

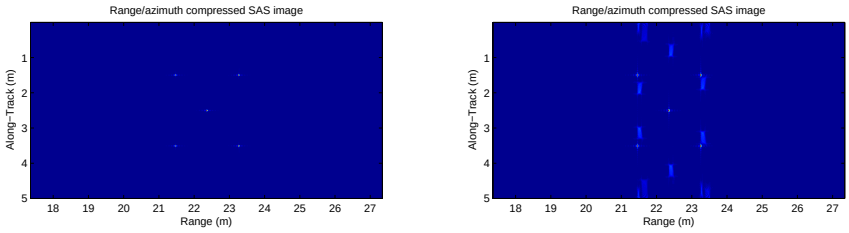

(a) No alias, PRF = 50 Hz, BW = 40kHz

(b) Alias in the along-track dimension, PRF = 2.5 Hz, BW = 40kHz

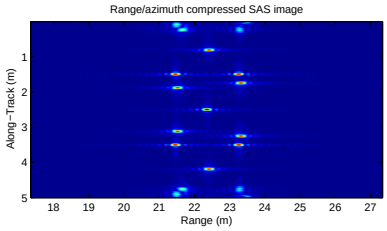

(c) Alias in the along-track dimension, PRF = 2.5 Hz, BW = 4kHz

Figure 5: SAS images produced using various pulse repetion rates.

Data is sampled in the pass-band domain (without any analogue frequency conversion). This allows for a

better phase accuracy of the recorded signal, which will be beneficial to the focusing and interferometric image formation algorithms. In this stage, the transducers response compensation can also be integrated as it is easier to compensate for a frequency dependent distortion in the signal as is received. Prior to the recording phase, the raw data is digitally converted to base-band (using the same DDS used for the output signal), filtered, decimated and, if desired, the raw echo data can be pulse compressed to further improve storage efficiency. Because we can treat FIR filters as a correlation between a desired impulse response and the input data, the correlation necessary for the pulse compression can be performed using the same digital processing structure as a FIR filter. The on-board PC receives the processed data and records it. The image formation algorithms and, in particular the along-track pulse compression, are executed after all the data is recorded. In the future it is expected to perform this task within the FPGA as to enable real time visualization of the survey data. One important aspect is the synchronization with the GPS data. To do this, time information obtained through the GPS receiver is used to correct the offset and frequency drift of a high precision and resolution clock implemented in the FPGA. This clock generates the output signal triggers that are consequently aligned with the GPS PPS signal. This echo data is time stamped using this precise clock.

4 Navigation subsystem

The accurate target area image formation process depends on the precise knowledge of the sensor position as it traverses the aperture. One of the major strengths of using a surface vessel is the use of satellite systems for navigation. Since the desired resolution is in the order of centimeters, this is the level of relative accuracy that is required for the vessel along the length of the synthetic aperture. This is possible with GPS navigation if operated in differential mode using carrier phase measurements. The long term errors of a CP-DPGS solution for a short baseline to the reference station is in the order of the decimeter; the short term errors, due to noise in the carrier phase tracking loops, is in the order of the centimeter. This error can further be smoothed out through integration of the GPS solution with inertial measurements. The ability of the boat to follow straight lines with small tracking errors has been proven in tests: less than half a meter of tracking error. This is more than enough for accurate image formation, given that motion error compensation algorithms are employed.

For height computation through In-SAS processing of pairs of images, precise attitude data has to be obtained so to precisely transform the lever between two sensors into target position estimate. For this purpose inertial sensor play a crucial role: through blending with the GPS data, it supplies pitch and roll estimates with levels of accuracy in the order of arcminutes; the heading error estimate is slightly poorer, but has less significant impact in the In-SAS processing algorithms.

The Navigation subsystem is basically a Kalman filter mixing the dynamic behavior of the vessel through the inertial sensor with the GPS reading. The major states are positioning, velocity and altitude (alignment) errors, but also includes inertial sensor biases. The output is a complete navigation solution, including position velocity and attitude information at a high data rate.

5 Image formation

Synthetic aperture sonar is a method for obtaining high resolution sonar images using simpler, smaller and lower cost transducer arrays. The successive displacement of the array is used to create a virtual array that can be several hundreds of meters long. After processing of the set of echoes, the image along-track resolution is in the order of the equivalent real array length and, in opposition to real aperture sonars, is maintained trough the entire range. Many algorithms have been developed to for SAS imagery ([3]). Currently two are being explored as to achieve the optimum results of the system: the Chirp Scaling Algorithm and the Inverse Scaled Fourier Transform. It is common to use the seismic or wave-number algorithm to obtain the synthetic aperture images. Recently the chirp-scaling algorithm has become more popular. The chirp-scaling algorithm avoids the burdensome non-linear interpolation by using the time scaling properties of the chirps that are applied in a sequence of multiplications and convolutions [5]. Nevertheless the chirp scaling algorithm is limited in use to processing of uncompressed echo data obtained by the transmission of chirp signals. A new approach based on the inverse scaled Fourier transform (ISFFT) [6] previously developed for the processing of SAR data is being followed. This algorithm interprets the raw data spectrum as a scaled and shifted replica of the scene spectrum. This scaling can then be removed during the inverse Fourier transformation if the normal IFFT is replaced by a scaled IFFT. This scaled IFFT

can be implemented by chirp multiplications in the time and frequency domain. The obtained algorithm is computationally efficient and phase preserving (e.g. fit for interferometric imagery). The model used for the formulation of the synthetic aperture image problem is illustrated in Figure 6.

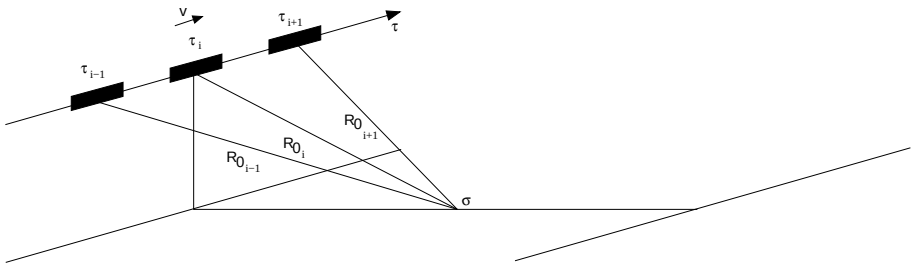

Figure 6: SAS model.

The point target response for this system is:

$$r_T(\tau_0, R_0,) = \sigma(\tau_0, R_0) \cdot s_T(t - t_v(\tau, R_0, \tau_0)) \cdot e^{-j2\pi f_0 \cdot t_v(\tau, R_0, \tau_0)} \cdot rect\left(\frac{\tau - \tau_c}{\Delta\tau}\right) \cdot e^{-j2\pi f \cdot t} \cdot e^{-j2\pi f_t au \cdot t} dt d\tau \tag{1}$$

Here $\sigma(\tau_0, R_0)$ is the backscatter intensity at the position (τ_0, R_0) and t_v the time delay related to the signal travel time across R_0. Using the Fourier transformation in both cross-track and along track dimension we get the point target spectra:

$$R_T(f, f_\tau) = S_T(f) \cdot rect\left(\left[\frac{f_\tau - f_c}{B_{AT}}\right]\right) \cdot \frac{\sqrt{\frac{c}{2}} \cdot \frac{1}{v} \cdot (f + f_0) \cdot e^{-j\pi/4}}{\left[(f + f_0)^2 - \frac{f_\tau^2 \cdot c^2}{4 \cdot v^2}\right]^{3/4}} \cdot \int\int_\infty \sqrt{R_0} \cdot \sigma(R_0, \tau_0) e^{-j2\pi f_\tau \tau_0} \cdot e^{-j4\pi \frac{R_0}{c} \sqrt{(f+f_0)^2 - \frac{f_\tau^2 \cdot c^2}{4 \cdot v^2}}} \cdot dR_0 \cdot d\tau_0 \tag{2}$$

$S_T(f)$ is the low-pass spectrum of the transmitted signal, f is the range frequency and f_τ is the along-track frequency. The complete scene raw echo data can be obtained describing the received backscatter delay as $t_v(\tau, R_0, \tau_0) = \frac{2R(\tau)}{c}$, substituting $R_0 = R_m + r$ and integrating the point scatter through the entire scene using the superimposition integral and performing some approximation steps. In SAR data one can approximate $\sqrt{R_0} = \sqrt{R_m + r} \approx \sqrt{R_m}$, because the mean range is many orders of magnitude higher than the scene range. In SAS data however, the average distance is of the order of the scene distance. This is reflected as an amplitude weighting dependent on range presented on the scene spectrum. Since this weighting is dependent only on range, its compensation can be included in the range compression step or prior to synthetic aperture image formation. The whole scene spectrum is hence:

$$R_T(f, f_t au) = S_T(f) \cdot rect\left[\frac{f_\tau - f_c}{B_{AT}}\right] \cdot \frac{f + f_0}{\left[(f + f_0)^2 - \frac{f_\tau^2 \cdot c^2}{4 \cdot v^2}\right]^{3/4}} \cdot e^{-j\pi/4} \cdot \sqrt{\frac{c}{2}} \cdot \frac{1}{v} \cdot \sigma(f_r(f, f_\tau), f_\tau) \tag{3}$$

Because we need a linear function of f and f_τ to invert the Fourier transform, the goal is to approximate the function $f_r(f, f_\tau) = \frac{2}{c}\sqrt{(f + f_0)^2 - \frac{f_\tau^2 \cdot c^2}{4 \cdot v^2}}$ by a first order Taylor decomposition given by:

$$f_r(f, f_\tau) = a(f_\tau) \cdot f + b(f_\tau) \cdot f_0 \tag{4}$$

Where $a(f_\tau) = \frac{2}{c}\frac{1}{\sqrt{1-\frac{f_\tau^2 \cdot c^2}{4v^2}}}$ and $b(f_\tau) = \frac{2}{c}\sqrt{1-\frac{f_\tau^2 \cdot c^2}{4v^2}}$. This approximation was found to be valid for SAR data, but is also valid for SAS data, where the propagation velocity is much lower, the center frequency is also lower and the center frequency to bandwidth ratio is quite higher than in SAR. As can be seen by the error surface depicted in Figure 7, this assumption is applicable still.

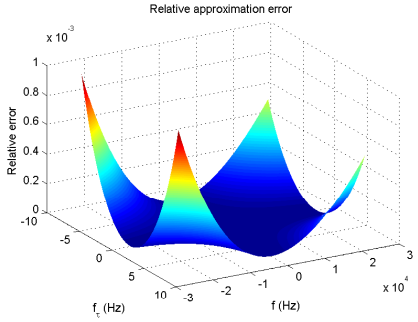

Figure 7: Approximation error.

The along-track focusing is carried out using the scaled Fourier transform [7], noting that:

$$\frac{1}{|a|} \cdot s(t) = \int_{-\infty}^{\infty} S(a \cdot f) \cdot e^{j2\pi a f t} \cdot df = F^{-1}\left\{S(a \cdot f)\right\} \tag{5}$$

After these steps, the desired synthetic aperture image is obtained by inverse Fourier transform in the f_τ dimension obtaining the desired image. An example of a SAS image can be seen in Figure 8, where 5 point targets obtained by simulation of the received raw echo data using the parameters of our sonar system and processing through the described ISFFT algorithm can be found.

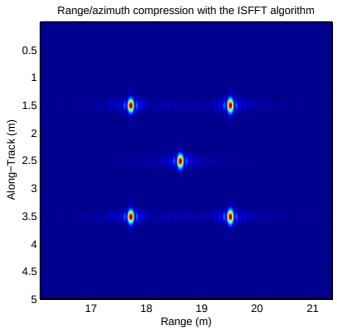

Figure 8: SAS Image.

Motion compensation can be applied to the acquired data in two levels: compensation of the known trajectory deviations and fine corrections trough reflectivity displacement, autofocus or phase-retrieval techniques ([8]). Because we are using an autonomous boat equipped with high precision navigation sensors, it is possible to use the first to correct most of the motion errors. If we assume that trajectory deviations cause range only variant aberrations, as is the case for large radiation pattern transducers and low magnitude attitude errors, they can be compensated in the form of a phase correction and a range shift in a pre-processing step. Velocity variations can be regarded as sampling errors in the along-track direction, and compensated through resampling of the original data. Nevertheless, as to achieve high quality images suitable for interferometry, it is the opinion of authors that fine corrections are still necessary, and so autofocus techniques should be applied to the data corrected by this first compensation stage.

Elevation maps can be obtained using interferometry techniques described in [7] and [9]. These are created by registration of a set of images and phase unwrapping of the resulting phase difference image. The

interferometry process can be helped by the fact that these images have embedded navigation data and so make the image registration tasks easier. Also because of the motion correction a higher correlation between images is obtained and so better quality interferograms are possible, yielding better results.

6 Project Status

At the present moment, the hardware of the SAS system (electronics, FPGA and interface) are concluded and being fully tested. The autonomous boat is also operational. Software for processing the acquired data has also been developed, although not having been designed for automated operation yet.

A couple of field tests have already been performed: one in the pool to test that all subsystems are operating well together; and other in a river, to acquire real world data. A problem with the signal amplifier and a poor choice of the target area rendered the obtained measurements to be of minor interest; if proved, however, that the system is well designed and will exhibit its full potential in the near future.

References

[1] Knight, W., 1981 Digital Signal Processing for Sonar. Proceedings of the IEEE, Vol. 68, NO. 11.

[2] Brunner, E., 2002. Ultrasound System Condiderations and their Impact on Front-End Components. Analog Devices.

[3] Gough, P. T., 1997. Unified Framework for Modern Synthetic Aperture Imaging Algorithms. The International Journal of Imaging Systems and Technology, Vol. 8, pp. 343-358.

[4] Lawlor, M. A. 1994. Methods for Increasing the Azimuth Resolution and Mapping Rate of a Synthetic Aperture Sonar. OCEANS '94. Proceedings, Vol. 3, pp. III/565-III/570, Brest, France.

[5] Runge, H., 1992. A Novel High Precision SAR Processor Based Chirp Scaling. International Geoscience and Remote Sensing Symposium, Vol. 1, pp. 372-375.

[6] Loffeld, Otmar, 1998. SAR Focusing: Scaled Inverse Fourier Transformation and Chirp Scaling. IEEE International Geoscience and Remote Sensing Symposium IGARSS, Seattle, USA.

[7] Hein, A., 2004. Processing of SAR Data: Fundamentals, Signal Processing, Interferometry. Springer.

[8] Fornaro, G., 1999. Trajectory Deviations in Airborne SAR: Analysis and Compensation. IEEE Transactions on Aerospace and Electronic Systems, Vol. 35, NO. 3.

[9] Griffiths, H. D., 1997. Interferometric synthetic aperture sonar for high-resolution 3-D mapping of the sea bed. IEE Proc.-Radar, Sonar Navig., Vol. 144, NO. 2.